Supplementary Information
Thermal Conductivity at Solid/Fluid interfaces: From Adsorption to Phonon Scattering through the Rattle Effect

Nikolas Ferreira de Souza[a,b], Cecilia Herrero[c], Thomaz Rossetti Ghizoni[a,b], Luís Fernando Mercier Franco[a], Benoit Coasne[b,c]

[a]University of Campinas, School of Chemical Engineering, Department of Chemical Systems Engineering, 13083-852 Campinas, Brazil
[b]Univ. Grenoble Alpes, CNRS, LIPhy, F-38000 Grenoble, France
[c]Institut Laue Langevin, F-38042 Grenoble, France

1 Force Field Parameters

The intermolecular interactions in the simulations were modeled using a combination of the Lennard-Jones (LJ) and Born-Mayer-Huggins (Born) potentials, along with Coulombic interactions for charged species. The details and references to each work are described in the methods sections of the main text. The potential styles `lj/cut` and `born/coul/long` follow the naming convention used in the LAMMPS documentation.[1]

The Lennard-Jones potential is given by:

$$U_{\mathrm{LJ}}(r) = 4\varepsilon \left[\left(\frac{\sigma}{r}\right)^{12} - \left(\frac{\sigma}{r}\right)^{6} \right], \tag{1}$$

where ε (in kcal/mol) is the depth of the potential well, σ (in Å) is the finite distance at which the interparticle potential is zero, and r is the interatomic distance. The Born-Mayer-Huggins potential, used to describe the short-range repulsion and Coulombic interactions, is given by:

$$U_{\mathrm{Born}}(r) = Ae^{-r/\rho} - \frac{C}{r^6} + \frac{D}{r^8} + \frac{q_i q_j}{4\pi\varepsilon_0 r}, \tag{2}$$

where A (in kcal/mol), ρ (in Å), C (in kcal·Å^6/mol), and D (in kcal·Å^8/mol) are empirical parameters. The last term represents the Coulombic interaction, where q_i and q_j are the atomic charges (in units of the elementary charge e), and ε_0 is the permittivity of vacuum. Bonded interactions were described using a harmonic potential:

$$U_{\mathrm{bond}}(r) = k(r - r_0)^2, \tag{3}$$

where k (in kcal/mol·Å^2) is the bond stiffness constant and r_0 (in Å) is the equilibrium bond length. The parameters used in the simulations are summarized in Tables (1), (2) and (3).

Table 1 Non-bonded interaction parameters used in the simulations.

Interaction	Type	A (kcal/mol)	ρ (Å)	C (kcal·Å^6/mol)	D (kcal·Å^8/mol)	Cutoff (Å)
Si-Si	born/coul/long	72652.50	3.5069	0.0	14453.46	14.0
Si-O	born/coul/long	623322.75	1.9385	0.0	3415.30	14.0
O-O	born/coul/long	15210.86	3.8609	0.0	618.88	14.0
Si-H	born/coul/long	0.0	10.0	0.0	0.0	14.0
O-H	born/coul/long	0.0	10.0	0.0	0.0	14.0
Interaction	Type	ε (kcal/mol)	σ (Å)	-	-	Cutoff (Å)
Si-CH_4	lj/cut	0.2757	4.00	-	-	14.0
O-CH_4	lj/cut	0.2647	3.214	-	-	14.0
CH_4-CH_4	lj/cut	0.294	3.73	-	-	14.0

Table 2 Bond parameters used in the simulations.

Bond Type	k (kcal/mol·Å^2)	r_0 (Å)
Si-O	495	0.945

Table 3 Atomic masses and charges used in the simulations.

Atom Type	Mass (g/mol)	Charge (e)
Si	28.0855	1.91042
O	15.999	-0.955209
O (sylanol)	15.999	-0.902605
H	1.00784	0.425
CH_4	16.04242	–

2 Comparison with the classical mixing rules

Figure S1 compares the effective thermal conductivity on the parallel direction, $\kappa^{\parallel}$, obtained from our molecular dynamics (MD) simulations with the values predicted by a classical mixing rule, as a function of the adsorbed amount N_{a}. A detailed interpretation of the results and their physical origin, as well as the implications for the validity of classical mixing approaches, is provided in the main text (Section 4.3).

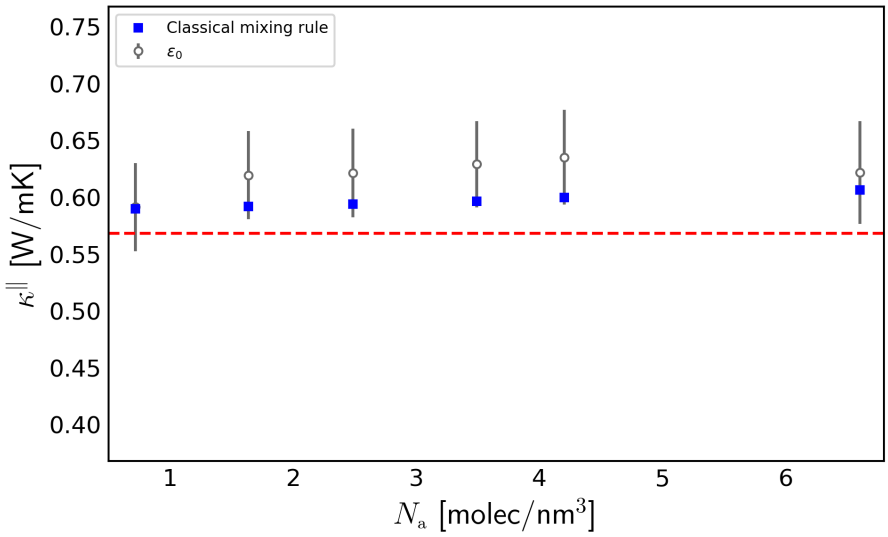

Figure S1 Effective parallel thermal conductivity of the fluid-filled silica pore. The different data sets show the results from molecular simulation and the prediction of a classical engineering mixing rule. The blue squares correspond to the classical mixing rule based on the volume fractions ϕ and intrinsic thermal conductivities κ° of the solid and fluid phases, *i.e.* $\kappa^{\parallel} = \phi_\alpha \kappa^{\circ}_\alpha + \phi_\beta \kappa^{\circ}_\beta \sim \phi_\beta \kappa^{\circ}_\beta$. Open circles represent simulation results for the nominal solid/fluid interaction strength ε_0. The dashed red line indicates the thermal conductivity of the empty pore as explained in the main text.

3 Thermal conductivity disentangling

The different contributions defined in Eq. (6) (from the main text) are shown in Fig. S2 as a function of the adsorbed layer density n_a. The solid contribution κ_β is found to be dominated by $\kappa_{\beta,\beta}$, which is constant and equal to the empty pore conductivity, while the negative cross-terms $\kappa_{\beta,\alpha}$ and $\kappa_{\beta,\alpha\beta}$ account for the reduction driven by the rattle effect. Similarly, κ_α is primarily governed by the fluid/fluid contribution $\kappa_{\alpha,\alpha}$ with additional contributions from the solid *beta* and the interface $\alpha\beta$. The interface contribution $\kappa_{\alpha\beta}$ is rather small since all terms related to the interface $\alpha\beta$ have a smaller magnitude compare to the others.

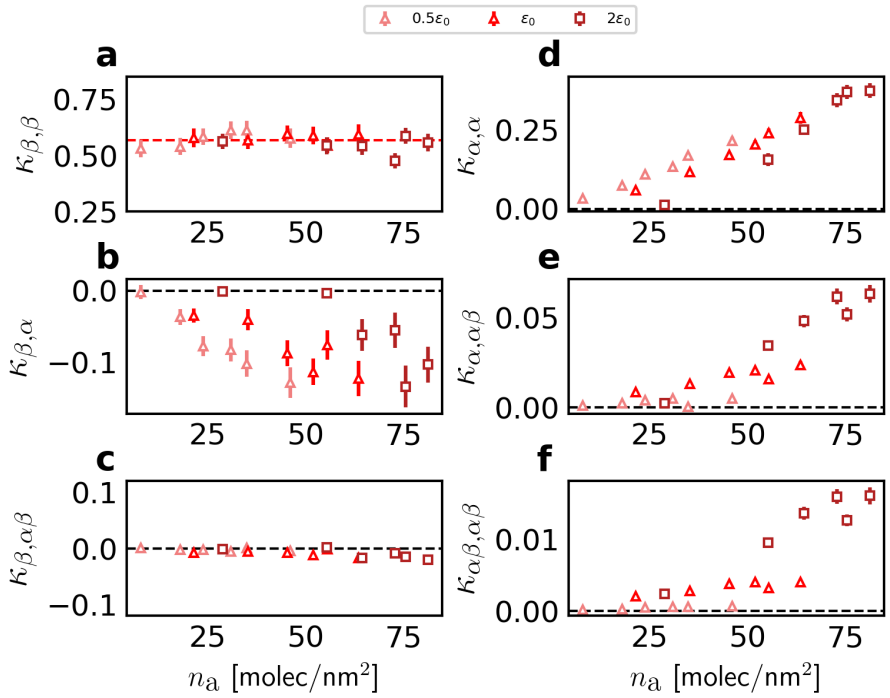

Figure S2 Contributions to the thermal conductivity.. Each of the six independent heat-current correlation terms contributing to Eq. (6) as a function of the adsorbed amount per unit surface area n_{a}. Panels (a–c) show the contributions involving the solid heat current, $\kappa_{\beta,\beta}$, $\kappa_{\beta,\alpha}$, and $\kappa_{\beta,\alpha\beta}$, while panels (d–f) show the corresponding contributions involving the fluid and interfacial heat currents, $\kappa_{\alpha,\alpha}$, $\kappa_{\alpha,\alpha\beta}$, and $\kappa_{\alpha\beta,\alpha\beta}$, respectively. Data are shown for three solid/fluid interaction strengths, $0.5\varepsilon_0$, ε_0, and $2\varepsilon_0$ (the legend is shown at the top of the panels). All thermal conductivity values are reported in units of W·m^{-1}·K^{-1}. The horizontal dashed line indicates zero thermal conductivity, while the red dashed line corresponds to the effective thermal conductivity of the empty pore, as discussed in the main text. Error bars represent statistical uncertainties and may be smaller than the marker in some data points.

References

[1] S. Plimpton, *J. Comput. Phys.*, 1995, **117**, 1–19.